Image Compression using All-optical DCT and DST

Bui Thi Thuy[1], Dang The Ngoc[2], Le Trung Thanh[3*]

[1]Hanoi University of Natural Resources and Environment
[2]Posts & Telecommunications Institute of Technology (PTIT)
[3]International School (VNU-IS), Vietnam National University, Hanoi
[*]Corresponding author: thanh.le@vnu.edu.vn
Received 7 July 2022; Revised 22 August 2022; Accepted 24 August 2022; Published 28 October 2022.
DOI: https://doi.org/10.54939/1859-1043.j.mst.82.2022.159-166

ABSTRACT

In this paper, we present a method for realizing all-optical Discrete Sine and Cosine Transform (DST/DCT) for image compression. We show that all-optical DST and DCT can be achieved by using only one 4x4 MMI (multimode interference) coupler at a suitable width and length. The proposed method can process image data at high speed and high bandwidth. We use numerical methods for simulating the whole devices

Keywords: All-optical discrete cosine transform (DCT); Image processing; Multimode interference coupler; Optical signal processing; Signal processing.

1. INTRODUCTION

Optical techniques have been considered for a variety of signal processing tasks, such as pattern recognition, the generation of ambiguity surfaces for radar signal processing, and image processing applications [1, 2]. The major reason for using an optical signal processor is its high bandwidth advantage over electronic processors. Due to its high throughput, the application of optical signal processing high performance computing systems is very attractive. Photonic signal processing transforms such as the discrete Fourier transform (DFT), discrete cosine transforms (DCT), and discrete wavelet transforms (DWT) are useful for spatial signal processing and optical computing such as spectrum analysis, filtering, encoding, etc.

In recent years, signal processing tasks in the optical domain used lens systems [3, 4], directional couplers [5, 6], and single mode star networks [7]. However, the systems based on these technologies are usually quite large, lack accuracy, and require high precision mechanical placement. In addition, the structure for implementing the transforms based on fiber technology requires bulky crossovers of fiber cables. Recently, the design of DFT and DCT transforms using fiber directional couplers has been presented by Moreolo and Cincotti [8]. In the literature [9, 10], a few transforms, such as Hadamard transforms and discrete unitary transformations, have employed MMI structures and multimode waveguide holograms. However, these devices were designed for the InP material system. For the device using holograms, a complex fabrication process is required. The presence of holograms within the multimode waveguide tends to introduce additional losses.

Recently, the methods for realizing all-optical Fourier transform based on multimode interference have been reported [11]. The design of these devices has been implemented on the silica material system. In addition, all-optical discrete cosine transforms and discrete sine transform using multimode interference couplers have been realized [12]. However, these structures still need to use fiber optic directional couplers.

In addition, recent research on all-optical image processing based on integrated optics has been carried out [13]. However, only Haar transform using directional couplers for image compression has been investigated. In addition, data compression supports to reduce the use of many expensive resources. In recent years, artificial intelligence (AI) algorithm implementation has continued to rely on electronic computing systems. The early neural networks relied on

standard CPU designs for computing, which were incapable of meeting the requirements of extremely large data sets. In addition, the parallel computing efficiency was low, necessitating the replacement of a GPU capable of parallel computing. GPUs facilitate the development of deep learning and AI in practice. However, classical deep learning has a bottleneck due to the high-speed processing of electrical inputs.

The researchers are attempting to find out other methods to solve electronic defects. One of the most promising answers to solve problems with data transportation is photonic interconnects or all-optical computing systems [14]. At practically every level of the computing hierarchy, photonic linkages have already supplanted metallic ones for the transfer of information at light speed, and they are currently being investigated for integration at the chip size.

While the DST and DCT are used as a sum of cosine functions that oscillate with different frequencies to express data points in a finite sequence. It has wide-ranging applications in computer engineering, such as MP3 compressing audio and JPEG image compression with cosine compared with sine functions, but few cosine functions can be used for signal approximation in order to efficiently express boundary conditions for differential equations [15]. DCT is used in video and image compression because various algorithms are developed to make DCT computationally effective and implemented with the DCT to reduce complexity by using rid of multiplication for approximation. Numerous image processing applications, such as tracking, required a larger DCT. DCT approximation has characteristics such as low complexity, low error energy, and high length of DCT for supporting the most recent video coding methods as well as other applications such as surveillance, encryption, tracking, encryption, and compression.

However, the present DCT algorithms cannot work efficiently for all the mentioned features due to the limitation of computing systems in the electronic domain. It is attractive to implement the DST and DCT for big data applications, especially as they apply to huge data sets. The use of ARM processors in FPGAs and the transfer of FPGAs towards heterogeneous computing platforms [16]. Therefore, in this paper, we propose a new method to realize all-optical DST and DCT based on multimode interference (MMI) structures using silicon waveguides for image processing applications. The proposed method is very attractive due to the advantages of low loss, ultra-compact size, and excellent fabrication tolerances. [17, 18].

2. THEORY OF ALL-OPTICAL DCT AND DST TRANSFORMS

The conventional MMI coupler has a structure consisting of a homogeneous planar multimode waveguide region connected to a number of single mode access waveguides. Figure 1 shows a structure of a rectangular 4x4 DST and DCT transform using only one 4x4 MMI coupler. Here, W_{MMI} and L_{MMI} is the width and length of the MMI coupler.

Figure 1. *The structure of the DST and DCT using a 4x4 MMI coupler.*

The self – imaging principle is background for optical MMI coupler's operation [17,18]. A multimode waveguide has a very important property that is self – imaging. The property allows input field can be reproduced in single or muiltiple images at periodic intermission along the waveguide's propagation direction.

The central structure of the MMI filter is formed by a waveguide designed to support a large number of modes.

In this paper, the access waveguides are identical single mode waveguides with width W_a.

The input and output waveguides are located at

$$x = \left(i + \frac{1}{2}\right)\frac{W_{MMI}}{N}, \quad (i = 0,\ 2,\ \ldots,\ N-1) \tag{1}$$

The electrical field inside the MMI coupler can be expressed by [19]:

$$E(x,z) = \exp(-jkz)\sum_{m=1}^{M} E_m \exp\left(j\frac{m^2\pi}{4\Lambda}z\right)\sin\left(\frac{m\pi}{W_{MMI}}x\right) \tag{2}$$

where $k = 2\pi n/\lambda$, λ is the operating wavelength, n is the waveguide refractive index and M is the total number of guided modes in the MMI coupler, E_m is the summation coefficients. It is assumed that the length of the MMI coupler is set to $L_{MMI} = 2\Lambda/N$, where $\Lambda = nW_{MMI}^2/\lambda$. The matrix characteristic of the MMI with suitable phase shifters at the input and output ports can be rewritten by:

$$T_{uv} = je^{j\frac{\pi}{4}}\sqrt{\frac{2}{N}}\sin\frac{\pi\left(u+\frac{1}{2}\right)\left(v+\frac{1}{2}\right)}{N} \tag{3}$$

This is the matrix of the DCT and DST transform. For N=4, we can achieve the matrix of the DST as follows:

$$M_{DST} = \begin{bmatrix} 0.1379 & 0.3928 & 0.5879 & 0.6935 \\ 0.3928 & 0.6935 & 0.1379 & -0.5879 \\ 0.5879 & 0.1379 & -0.6935 & 0.3928 \\ 0.6935 & -0.5879 & 0.3928 & -0.1379 \end{bmatrix} \tag{4}$$

Therefore, the matrix of equation (3) is the matrix of the DST-IV if the phase factor $j\exp(j\frac{\pi}{4})$ is neglected. Also, the matrix of the DCT-IV can be expressed by:

$$M_{DCT} = \sqrt{\frac{2}{N}}\cos\frac{\pi\left(u+\frac{1}{2}\right)\left(v+\frac{1}{2}\right)}{N} \tag{5}$$

$$M_{DCT} = \begin{bmatrix} 0.6935 & 0.5879 & 0.3928 & 0.1379 \\ 0.5879 & -0.1379 & -0.6935 & -0.3928 \\ 0.3928 & -0.6935 & 0.1379 & 0.5879 \\ 0.1379 & -0.3928 & 0.5879 & -0.6935 \end{bmatrix} \tag{6}$$

Therefore, the DCT-IV can be implemented using the DST –IV device based on MMI structures by putting a phase shifter π at the even input ports and re-labeling all the output ports with the inverse order.

In digital format, two-dimensional images are a collection of millions of pixels, each of which is represented by a series of bits. These photos are raster or bitmapped as opposed to vector images, which use mathematical formulas to produce geometric objects. As the demand for higher-quality photographs and movies grows, attempts have been made to raise the image storage resolution [20]. When sharing a lot of images at the same time, it causes to increase transmission bandwidth and transmission time. In addition, there are many disadvantages when storing images on web servers such as: wasting storage space, increasing load time, making customer experiences. To slove this problem, images compression is the best solution that is

efficient for sharing, viewing, transmissing a large mount of imanges. DCT and DST, therefore, have been utilized in voice and image processing for compression, filtering, and feature extraction throughout the past decade. Using DCT, an image can be broken down into its component parts. DCT expresses a sequence of finitely many discrete and real data points with equal symmetry by summing cosine functions oscillating at different frequencies.

Figure 2 illustrates the processing stages at the core of the DCT-based modes of operation. These images depict a particular instance of single-component (grayscale) image compression. The reader may comprehend the essence of DCT-based compression by seeing it as the compression of a stream of 8x8 blocks of grayscale image samples. Multiple grayscale images are compressed either totally one at a time or by interleaving 8x8 sample blocks from each image in the sequence. Each 8x8 block is input, traverses each processing step, and gives output in compressed form into the data stream. For DCT progressive-mode codecs, an image buffer exists before the entropy coding process, allowing an image to be stored and subsequently divided into numerous scans with progressively better quality.

The DST and DCT convert image data into its equivalent frequency domain by partitioning the image pixel matrix into blocks of size N x N, N depending upon the type of image. For example, if we used a black & white image of 8 bit then all shading of black & white color can be expressed into 8 bit hence we use N = 8, similarly for the color image of 24 bit we can use N = 24 but using block size N = 24, time complexity may increase. In this study, we consider the block of 4x4 by using 4x4 MMI coupler.

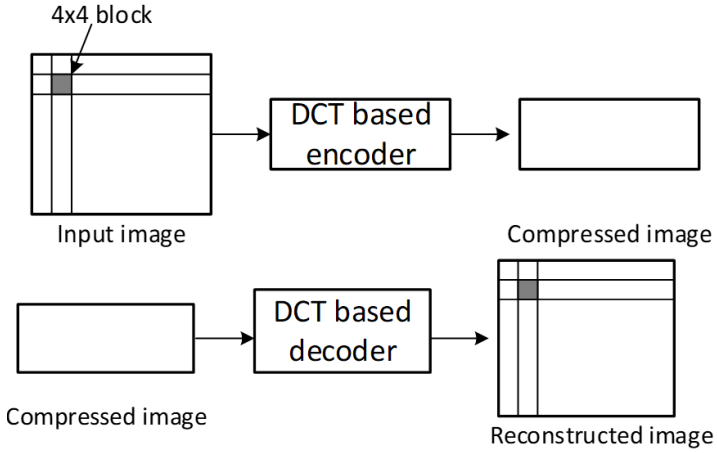

Figure 2. *Principle of image compression and de-compression based on the DCT [20].*

3. RESULTS AND DISCUSSION

In this section, we design the all-optical DCT and DST transform using numerical simulations. The material Si3N4 working at visible wavelengths RGB color is used for image processing. The height and width of the waveguide are $h_{co} = 170nm$ and $W_a = 1600nm$, respectively (figure 3). The calculated effective refractive index is to be $n_{eff} = 1.7$. For the MMI region, we still use the same waveguide structure but with a wider width W_{MMI} to support higher order modes.

The numerical simulation results for the 4x4 MMI design are shown in figure 4. The optimal length and width of the 4x4 MMI were calculated to be 708 µm and 24 µm. Figure 4(a), (b), (c) and (d) shows for input data $(x_0 x_1 x_2 x_3)^T$ = (1000), (0100), (0010) and (0001), respectively. Here, the power is represented by the gray level of a pixel in the image. The output amplitudes and phases at the output ports are calculated by using numerical methods.

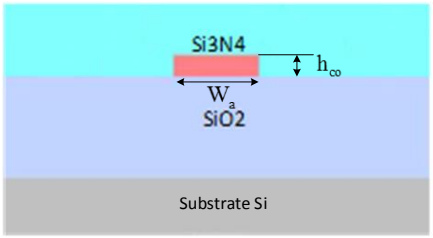

Figure 3. *Waveguide structure.*

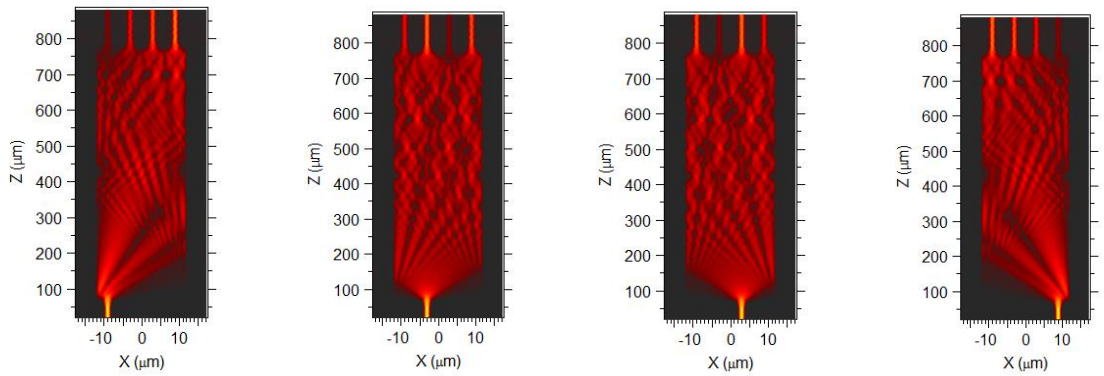

(a) *(b)* *(c)* *(d)*

Figure 4. *Simulation result of the DCT for different image data.*

For all-optical signal processing, the DST and DCT formed from the 4x4 MMI structure of figure 1 can be expressed by the following matrix:

$$H_{6x6MMI} = \begin{bmatrix} \alpha e^{j\pm\delta} & \alpha e^{j\pm\delta} & \alpha e^{j\pm\delta} & 0 \\ \alpha e^{j\pm\delta} & \alpha e^{j\pm\delta} & -\alpha e^{j\pm\delta} & 0 \\ \alpha e^{j\pm\delta} & -\alpha e^{j\pm\delta} & \alpha e^{j\pm\delta} & \alpha e^{j\pm\delta} \\ \alpha e^{j\pm\delta} & -\alpha e^{j\pm\delta} & 0 & -\alpha e^{j\pm\delta} \end{bmatrix} \quad (7)$$

Where α and δ are variations in amplitude and phase around 1 and 90 degrees. In the next section, we show that our proposed architecture can provide a very high fabrication tolerance. As a result, the Haar transform can be implemented accurately. The bock of 4 bits in image signals is represented at input ports In1, In2, In3, and In4. The processed signals after the DST and DCT transform are presented at output ports Out1, Out2, Out3, Out4.

The normalized powers of the DCT matrix can be expressed by:

$$H_{DCT} = \begin{bmatrix} 0.4810 & 0.3457 & 0.1543 & 0.0190 \\ 0.3457 & 0.0190 & 0.4810 & 0.1543 \\ 0.1543 & 0.4810 & 0.0190 & 0.3457 \\ 0.0190 & 0.1543 & 0.3457 & 0.4810 \end{bmatrix} \quad (8)$$

The normalized powers at output ports 1-4 when the input signal is at 1, 2, 3, and 4 are shown in figure 5. The simulations show that the length variation of ±2 μm still keeps the output powers unchanged. This means that the fabrication tolerance of the proposed structure is high. The current CMOS fabrication technology for the VLSI industry is feasible.

Next, we investigate the phase error of the DST and DCT transforms. The phases at output ports 1-4 when the input signal is at port 1 are shown in figure 6. The exact phase can be obtained over a length variation of 18 μm. This result provides a flexible design for the optical DST/DCT. The

DST/DCT can be implemented extremely accurately using the CMOS fabrication technology.

Next, we undertake the simulations for the input image of the "camera man", 256x256 in size, at different compressed ratios of 10%, 20%, 70%, and 90% with the optical DCT Transform architecture designed above. The simulation results are shown in figure 7.

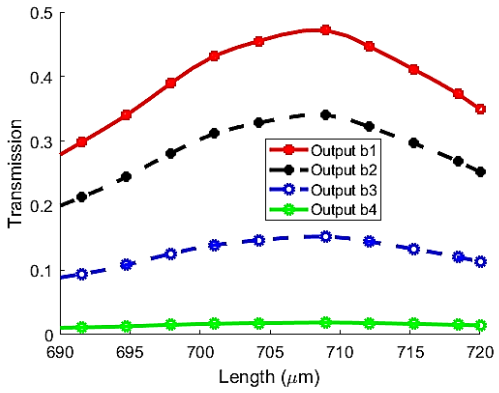

Figure 5. *Normalized powers at output ports around the optimal length.*

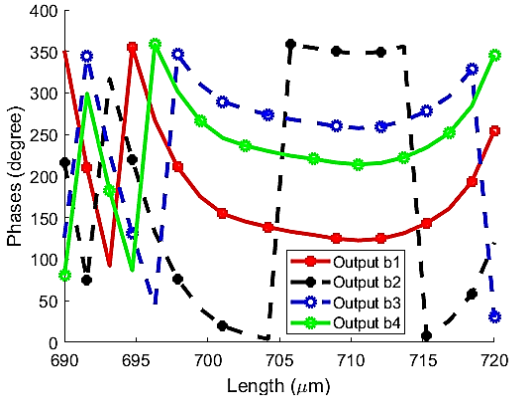

Figure 6. *Phase at output ports of the DCT/DST transform based on 4x4 MMI coupler.*

(a) "Camera man" image, CR = 90%.

(b) "Camera man" image, CR = 70%.

(c) "Camera man" image, CR = 20%.

(d) "Camera man" image, CR = 10%.

Figure 7*. Original and compressed images.*

As an example, we show the results for compressed images compared to the original image with different compressed ratios (CR) in figure 7. The most well – known measure of quality of reconstrution in lossy compression is PSNR. It is ratio bewteen the signal and noise. In image compression, the signal is orginal images and the noise is the error that is introduced by compression. The below formula determines value of the PSNR.

$$PSNR\ [dB] = 10Log_{10}(\frac{255^2}{MSE}) \tag{9}$$

The mean squared error (MSE) is defined as the mean of the square of the difference between the original and reconstructed pixels. As a loss function, As MSE increases, the image quality degrades. The MSE between two images f and g (size MxN) can be expressed by:

$$MSE = \frac{1}{MxN}\sum_{j=1}^{N}\sum_{k=1}^{M}\left[f(j,k) - g(j,k)\right]^2 \tag{10}$$

Table 1 presents the comparison of the MSE, PSNR, and the images compressed by using the all-optical DCT transform. Increasing PSNR represents the increasing fidelity of compression. When both images are identical, MSE=0, the PSNR is undefined.

Table 1. *Image compression results for the cameraman's image.*

CR (Compressed Ratio)	PSNR (dB)	MSE
10%	77	0.0012
20%	75	0.002
70%	70	0.062
90%	66	0.075

4. CONCLUSIONS

We have proposed a new method for realizing all-optical DST and DCT transforms using only one 4x4 MMI coupler for image compression. The designs of the proposed devices have been performed using numerical methods. The DST and DCT have been successfully designed in the Si3N4 material platform, which is suitable for VLSI and FPGA circuits. This all-optical approach for the DST/DST realization can be useful for all-optical high-speed and real-time image processing applications such as data compression, filtering, and coding. The method can also be useful for the integration of fast image processing into the AI camera in the future.

REFERENCES

[1]. A. VanderLugt, *"Optical signal processing"*. New York: J. Wiley & Sons, (1992).
[2]. N. B. Le, *"Photonic signal processing: techniques and applications"*. CRC Press, (2007).
[3]. J. W. Goodman, A. R. Dias, and L. M. Woody, *"Fully parallel, high-speed incoherent optical method for performing discrete Fourier transforms,"* Optics Letters, vol. 2, no. 1, pp. 1-3, (1978).
[4]. D. G. Sun, N. X. Wang, and L. M. H. e. al., *"Butterfly interconnection networks and their applications in information processing and optical computing: applications in fast-Fourier-transform-based optical information processing,"* Appl. Opt., vol. 32, no. 35, pp. 7184-7193, (1993).
[5]. A. E. Siegman, *"Fiber Fourier optics,"* Optics Letters, vol. 26, no. 16, pp. 1215-1217, (2001).
[6]. G. Cincotti, *"Fiber wavelet filters,"* IEEE Journal of Quantum Electronics, vol. 38, no. 10, pp. 1420-1427, (2002).
[7]. M. E. Marhic, *"Discrete Fourier transforms by single-mode star networks,"* Optics Letters, vol. 12, no. 1, pp. 63-65, (1987).
[8]. M. S. Moreolo and G. Cincotti, *"Fiber optics transforms,"* in 10th Anniversary International Conference onTransparent Optical Networks (ICTON 2008), Athens. Greece, (2008).

[9]. A. R. Gupta, K. Tsutsumi, and J. Nakayama, *"Synthesis of Hadamard Transformers by Use of Multimode Interference Optical Waveguides,"* Appl. Opt., vol. 42, pp. 2730-2738, (2003).
[10]. S. Tseng, Y. Kim, C. J. K. Richardson, and J. Goldhar, *"Implementation of discrete unitary transformations by multimode waveguide holograms,"* Appl. Opt., vol. 45, no. 20, pp. 4864-4872, (2006).
[11]. J. Zhou, *"Realization of Discrete Fourier Transform and Inverse Discrete Fourier Transform on One Single Multimode Interference Coupler,"* IEEE Photonics Technology Letters, vol. 23, no. 5, pp. 302 - 304, (2011).
[12]. J. Zhou and M. Zhang, *"All-Optical Discrete Sine Transform and Discrete Cosine Transform Based on Multimode Interference Couplers,"* IEEE Photonics Technology Letters, vol. 22, no. 5, pp. 317 - 319, (2010).
[13]. L. Almeida, N. Kumar, G. Parca, A. Tavares, A. Lopes, and A. Teixeira, *"All-Optical image processing based on integrated optics,"* 16th International Conference on Transparent Optical Networks (ICTON), vol. DOI: 10.1109/ICTON.2014.6876660, (2014).
[14]. F. P. Sunny, E. Taheri, M. Nikdast, and S. Pasricha, *"A Survey on Silicon Photonics for Deep Learning,"* J. Emerg. Technol. Comput. Syst., vol. 17, no. 4, p. Article 61, (2021).
[15]. M. Deivakani, S. V. S. Kumar, N. U. Kumar, E. F. I. Raj, and V. Ramakrishna, *"VLSI Implementation of Discrete Cosine Transform Approximation Recursive Algorithm,"* Journal of Physics: Conference Series, vol. 1817, no. 1, p. 012017, (2021), doi: 10.1088/1742-6596/1817/1/012017.
[16]. R. Woods, J. McAllister, G. Lightbody, and Y. Yi, *"FPGA-based Implementation of Signal Processing Systems"*. Wiley, (2017).
[17]. M. Bachmann, P. A. Besse, and H. Melchior, *"General self-imaging properties in N x N multimode interference couplers including phase relations,"* Appl. Opt., vol. 33, no. 18, pp. 3905-, (1994).
[18]. L. B. Soldano and E. C. M. Pennings, *"Optical multi-mode interference devices based on self-imaging: principles and applications,"* IEEE Journal of Lightwave Technology, vol. 13, no. 4, pp. 615-627, (1995).
[19]. J. M. Heaton and R. M. Jenkins, *"General matrix theory of self-imaging in multimode interference (MMI) couplers,"* IEEE Photonics Technology Letters, vol. 11, no. 2, pp. 212-214, (1999).
[20]. J. John, *"Discrete Cosine Transform in JPEG Compression,"* https://doi.org/10.48550/arXiv.2102.06968

TÓM TẮT

Nén ảnh sử dụng biến đổi DST và DCT trong miền toàn quang

Bài báo đưa ra một phương pháp thiết kế bộ biến đổi sin và cosin rời rạc DST/DCT ứng dụng cho nén ảnh trong miền toàn quang. Nghiên cứu chỉ ra rằng, chỉ cần dùng một cấu trúc giao thoa đa mode với 4 cổng vào và 4 cổng ra với cấu trúc phù hợp có thể thực hiện được bộ biến đổi DST và DCT. Kết quả mô phỏng nén ảnh trong miền toàn quang cho thấy bộ biến đổi DCT và DST này xử lý dữ liệu ảnh ở tốc độ cao. Toàn bộ cấu trúc phần cứng được mô phỏng sử dụng các phương pháp số.

Từ khoá: Xử lý tín hiệu; Biến đổi tín hiệu; Biến đổi DCT/DST; Xử lý ảnh số; Nén ảnh; Xử lý dữ liệu toàn quang; Thông tin quang; Phần cứng máy tính.